



# Molecular beam laser spectroscopic studies of the photoactive properties of resveratrol

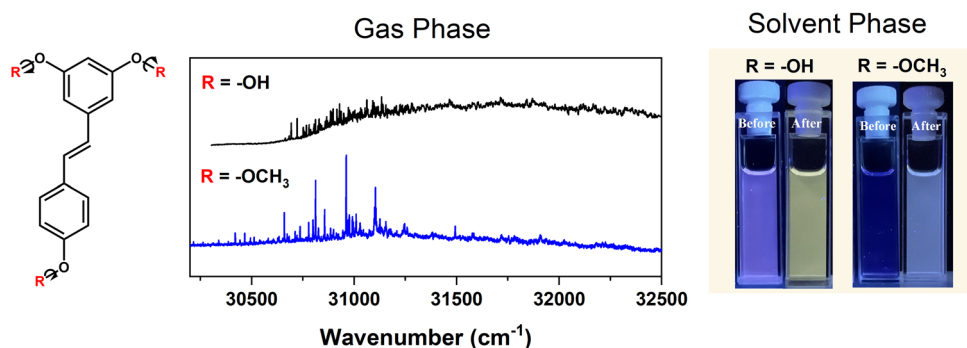
Jiayun Fan<sup>1</sup> · Wybren Jan Buma<sup>1,2</sup>

Received: 14 July 2023 / Accepted: 4 September 2023 / Published online: 3 November 2023  
© The Author(s) 2023

## Abstract

Resonance Enhanced MultiPhoton Ionization spectroscopic techniques coupled with laser desorption and supersonic cooling have been employed to elucidate the photoactive properties of resveratrol. The observed excitation spectra give evidence for an internal-energy dependent *trans*–*cis* isomerisation pathway in the electronically excited state, while pump-probe studies show dynamics that are in line with what is known for the parent compound, *trans*-stilbene. Similar studies have been performed on a derivative of resveratrol with methoxy instead of hydroxy groups, a compound aimed to reduce previously observed photodegradation pathways of resveratrol. Time-resolved studies of the latter compound under solution conditions have given further insight into its excited-state dynamics and support the isolated-molecule conclusions on the topology of the potential energy surface of the electronically excited state. Spectroscopic studies under prolonged irradiation conditions show that both compounds suffer from photodegradation, although in the alkylated compound other pathways appear to be involved than in resveratrol.

## Graphical abstract



**Keywords** Sunscreen filters · Electronic spectroscopy · Excited state dynamics · Molecular beams · Photochemistry · Quantum chemical calculations

## 1 Introduction

*Trans*-resveratrol (*E*-5-(4-hydroxystyryl)benzene-1,3-diol, Fig. 1) is a natural compound first isolated in 1939 from the root of the white hellebore [1] and mostly found in red grapes, berries, and nuts [2]. Although the compound initially received hardly any attention, this changed considerably when its cancer chemopreventive activity in stages of carcinogenes was discovered [3]. As of then, many studies

✉ Wybren Jan Buma  
w.j.buma@uva.nl

<sup>1</sup> Van 't Hoff Institute for Molecular Sciences, University of Amsterdam, Science Park 904, 1098 XH Amsterdam, The Netherlands

<sup>2</sup> Institute for Molecules and Materials, Radboud University, FELIX Laboratory, Toernooiveld 7c, 6525 ED Nijmegen, The Netherlands

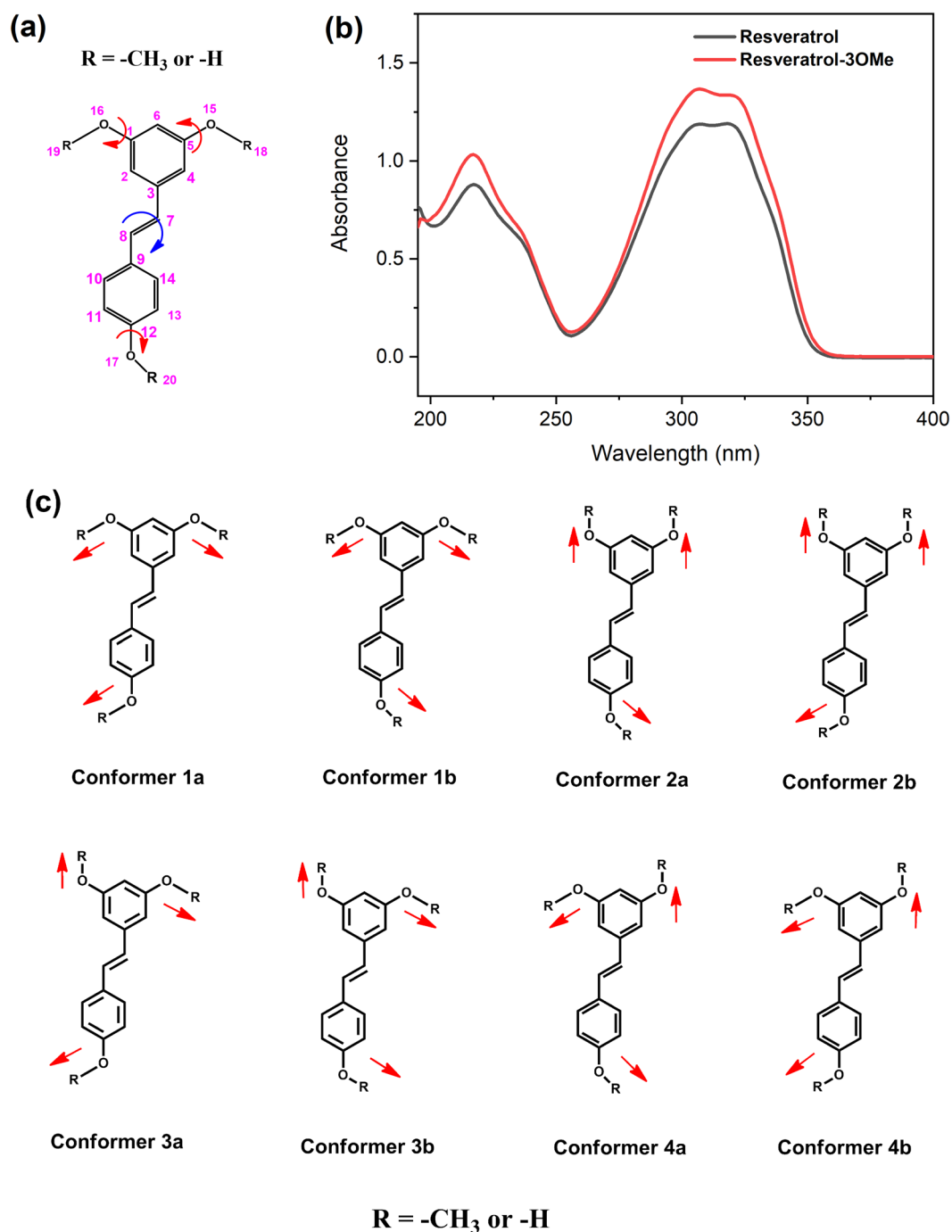


**Fig. 1** **a** Molecular structure of *trans*-resveratrol ( $R = -H$ ) and *trans*-resveratrol-3OMe ( $R = -OCH_3$ ). **b** UV absorption spectra of *trans*-resveratrol (black) and *trans*-resveratrol-3OMe (red) in ethanol at a

concentration of  $6 \times 10^{-6}$  mol/L. **c** Possible conformations of *trans*-resveratrol and *trans*-resveratrol-3OMe (color figure online)

started focusing on its pharmacological activities with currently more than 240 clinical trials that have been performed for its use in the treatment of chronic diseases, such as cancers, Alzheimer, diabetes, and others [4–8]. Apart from these pharmacological applications, *trans*-resveratrol has

also become quite well-known for its antioxidant properties [9, 10].

Another area for which *trans*-resveratrol has been considered to be of interest finds its origin in its spectroscopic properties. It is an effective UV absorber with a reduced human and ecological hazard, [11] and thus an excellent

starting point for applications such as UV filters in nature-based sunscreen formulations [12, 13]. However, detailed studies of the photochemical properties of *trans*-resveratrol showed that photon absorption is accompanied by photoisomerization and a wide variety of follow-up reactions leading amongst else to conversion into (*E*)-4-(6,8-dihydroxynaphthalen-2-yl)but-3-en-2-one (resveratrone) [14, 15] Photochemical isomerization by itself does not necessarily need to be too much of a drawback as long as the UV absorption properties are not dramatically altered, but follow-up reactions are in this respect more problematic. Such drawbacks combined with the limited solubility of the compound clearly are not favorable characteristics in a sunscreen context but also not from a biomedical point of view [15–17].

Despite these drawbacks, one can envision that substantial improvements in the photochemical profile of *trans*-resveratrol might be obtained using resveratrol as the core structure of novel compounds but substituting this core structure at strategically chosen positions with judiciously chosen chemical groups. One such an example—and the one that will be further explored in the present studies—is alkylation of the hydroxy groups as this should inhibit degradation to resveratrone according to the currently accepted degradation pathway to this compound [14, 15]. Key to such rational design attempts is a fundamental knowledge of the spectroscopic and decay dynamics of the electronically excited states involved in the absorption and energy dissipation of UV photons. As yet, such studies are rare [18–21]. In the present study we will provide such knowledge by Resonance Enhanced MultiPhoton Ionization (REMPI) laser spectroscopic studies on isolated compounds cooled in supersonic expansions. These studies are accompanied by studies under solvated conditions at room temperature focusing on the excited-state decay dynamics and the photostability of these compounds under such conditions.

## 2 Experimental details

### 2.1 Materials

*Trans*-resveratrol was purchased from Sigma-Aldrich and used without further purification. *E*-1,3-dimethoxy-5-(4-methoxystyryl)benzene (in the following referred to as *trans*-resveratrol-3OMe) was synthesized according to the procedure described below. Figure 1a, b displays the structure of the two compounds as well as their absorption spectra dissolved in ethanol at a concentration of  $6.0 \times 10^{-6}$  M.

*Trans*-resveratrol-3OMe To a solution of resveratrol (1.0 g, 4.38 mmol) in acetone (20 mL) was added  $K_2CO_3$  (5.45 g, 39.4 mmol) after which the reaction mixture was

stirred for 5 min. Next, iodomethane (2.45 mL, 5.59 g, 39.4 mmol) was added, after which the reaction mixture was stirred for 40 h at RT. TLC indicated complete conversion. The reaction mixture was poured into 150 mL ethyl acetate, washed with 50 mL 19% aqueous  $NH_4Cl$  and 50 mL brine, dried ( $Na_2SO_4$ ), and concentrated in vacuo to give 1.11 g. This was flash chromatographed ( $SiO_2$ , gradient EtOAc/petroleum ether 40–60 °C—5/95 → 10/90 → 15/85) to give 0.97 g of the title product.  $^1H$  NMR ( $CDCl_3$ , 400 MHz),  $\delta$  7.45 (d,  $J=8.6$  Hz, 2H), 7.04 (d,  $J=16.2$  Hz, 1H), 6.95–6.86 (m, 3H), 6.65 (d,  $J=2.2$  Hz, 2H), 6.38 (t,  $J=2.2$  Hz, 1H), 3.83 (s, 9H); TLC:  $R_f \approx 0.7$  (EtOAc/petroleum ether 40–60 °C—50/50).

*Trans*-resveratrol-3OMe was seeded into a supersonic expansion of 1.5 bar Ar and a pulse duration of 180  $\mu s$  by heating the compound to a temperature of 120 °C using a heatable valve (General Valve Iota One) with a 0.5 mm orifice diameter that was kept 5 °C higher than the main body to avoid clogging. The low vapor pressure of *trans*-resveratrol at elevated temperatures inhibited the heating of the compound to obtain a sufficiently high concentration in the molecular beam. Instead, a laser desorption source was employed to seed the compound in a 6 bar Ar expansion with pulse lengths of 34  $\mu s$  using a piezo valve (Amsterdam Cantilever Piezo valve [22]). To this purpose, a 1:1 in volume sample mixture of *trans*-resveratrol mixed with carbon powder was coated on a 55 cm EDM-AF graphite bar and desorbed by a 1064 nm IR beam from a Polaris pulsed Nd:YAG laser (New Wave Research) operating at 30 Hz and providing 1.5–2.0 mJ pulses. In both cases, the supersonic expansion passed through a 2.5 mm skimmer before entering the ionization chamber in which the REMPI experiments were performed.

Two-color (1 + 1') R2PI studies have been performed using the frequency-doubled output of a Sirah Precision Scan dye laser operating either on DCM or pyrromethene 597 and pumped by a Spectra-Physics Lab 190 Nd:YAG laser to excite molecules to electronically excited states, while ionization of these states took place using a Neweks PSX-501 ArF excimer laser (193 nm, 6.42 eV). Typical pulse energies of pump and probe lasers were 0.5–1 mJ and 1 mJ, respectively. Time-resolved pump-probe experiments were performed by delaying the output of the ArF laser using a Stanford Research Systems DG545 delay generator. To record UV depletion spectra, an additional laser system consisting of a Sirah Cobra-Stretch dye laser pumped by a Spectra-Physics Lab 190 Nd:YAG laser was employed. This laser system delivered 2–3 mJ laser pulses and was fired 150 ns before the excitation and ionization lasers.

Time-resolved emission studies have been performed using the Time-Correlated Single Photon Counting (TC-SPC) setup described previously [23]. In these experiments,

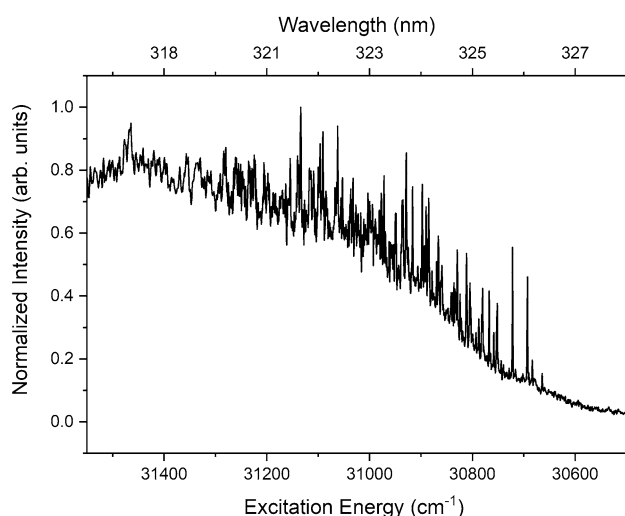


**Fig. 2**  $(1 + 1')$  R2PI excitation spectrum of *trans*-resveratrol

compounds were dissolved in ethanol concentration of  $6.0 \times 10^{-6}$  M. Similar samples were employed for the photostability studies for which a tunable Nd:YAG-laser system (NT342B, Ekspla) operating at 318 nm (the maximum of the absorption band) and delivering 1 mJ pulses with a pulse length of 5 ns at a repetition rate of 10 Hz was used to irradiate the sample for a certain amount of time after which it was analyzed.

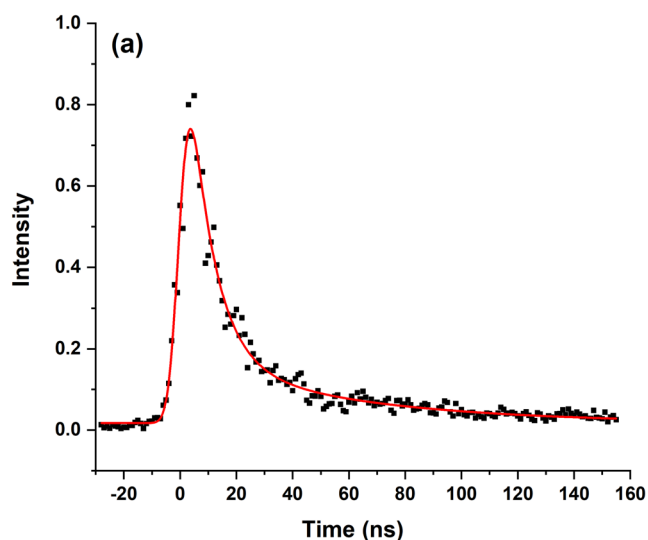


**Fig. 3** Decay curves of (a) *trans*-resveratrol and (b) *trans*-resveratrol-3OMe obtained after excitation at 30,664.0 and 30,184.6  $\text{cm}^{-1}$ , respectively. The red traces are fits of the decays to the convolution

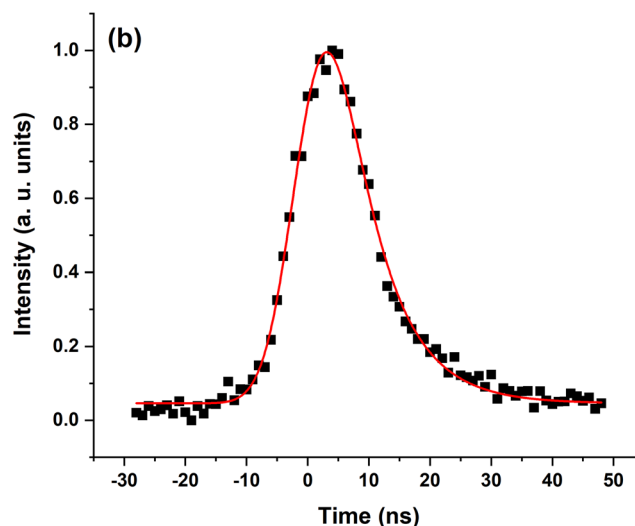
## 2.2 Theoretical

Geometry optimizations of ground and electronically excited states followed by calculations of the harmonic force field have been performed using Time-Dependent(TD)-Density Functional Theory at the wb97XD/cc-pVDZ level [24]. All calculations have been performed with the Gaussian16, Rev.C.01 suite of programs [25].

## 3 Results and discussion

### 3.1 Molecular beam studies

Figure 2 shows the  $(1 + 1')$  R2PI excitation spectrum of *trans*-resveratrol in the region from 30,500 to 31,500  $\text{cm}^{-1}$  (317.5–328 nm), while the excitation spectrum recorded over a much larger energy region is depicted in Fig. 3. To facilitate a direct comparison with the spectrum reported by de Vries et al. [18] this spectrum has been plotted as a function of increasing wavelength. In the previous study only the 325–326 nm region was reported as being the region where a sharp, well-resolved spectrum could be observed without an underlying absorption background. The present spectrum shows indeed a background signal that is increasing for higher excitation energies, but at the same time it is clear that at these energies there is extensive vibronic activity that can still be well-resolved. Equally interesting to notice is that the first resonance that is observed occurs at 30,664.0  $\text{cm}^{-1}$  (326.12 nm) with a



of a Gaussian profile with a biexponential decay of 9 ns (0.86) and 57 ns (0.14) for resveratrol, and a mono-exponential decay of 7 ns for resveratrol-3OMe, respectively

**Table 1** Relative energies ( $\text{cm}^{-1}$ ) of conformers of *trans*-resveratrol and *trans*-resveratrol-3OMe based on DFT calculations at the wb97XD/cc-pVDZ level

	1a	1b	2a	2b	3a	3b	4a	4b
Trans-resveratrol	263	165	341	409	312	197	0	142
Trans-resveratrol-3OMe	453	0	408	668	217	41	348	612

width of  $1.4 \text{ cm}^{-1}$ , thus just falling outside the region previously reported on.

In the previous ( $1 + 1'$ ) R2PI studies an ionization wavelength of 329 nm was used, which brought the total absorbed energy just above the ionization threshold. Comparison with the present spectrum—which has been obtained with an ionization laser at 193 nm—does not show significant differences. This suggests (i) that the potential energy surfaces of  $S_1$  and  $D_0$  are not significantly displaced from each other and (ii) that ionization predominantly takes place to  $D_0$  without significant contributions of ionization pathways to electronically excited states of the ion.

It is instructive to compare the excitation spectrum measured in the present study for *trans*-resveratrol with that of the parent compound *trans*-stilbene [26]. Such a comparison first of all leads to the conclusion that substitution with the three hydroxy groups leads to a red shift of the  $S_1 \leftarrow S_0$  excitation spectrum by  $1568 \text{ cm}^{-1}$ . As with respect to the vibrational activity, it is noticed that the excitation spectrum of *trans*-stilbene is dominated by the activity of low-frequency modes associated with the ethylenic  $C_e=C_e$  and  $C_e-C_{ph}$  torsions which become prominently visible due to their highly anharmonic character [26–29]. For excess vibrational energies above  $1200 \text{ cm}^{-1}$  bands become broader and the spectrum ultimately becomes entirely diffuse which has been attributed to the activation of *trans*–*cis* isomerisation in the excited state. Figure 2 appears to suggest that for *trans*-resveratrol such a blurring out might already occur at lower excess vibrational energies. This would imply that for this compound the barrier for *trans*–*cis* isomerization in the excited state is lower than that of the parent compound.

A detailed assignment of bands in the excitation spectrum of *trans*-resveratrol is more difficult. As can be concluded from Table 1 the compound has several low-energy conformers associated with the orientation of the hydroxy groups (see Fig. 1c) as a result of which the excitation spectrum might have contributions from more than a single conformer. We have tried to get further insight in this by performing depletion experiments. However, the signal-to-noise ratio that can be achieved in R2PI experiments in which seeding is performed with laser desorption is considerably worse than in experiments in which the compound can simply be heated. As a result, it was not possible to record depletion spectra that could address this issue. On the other hand, our studies

on *trans*-resveratrol-3OMe that will be discussed below definitely demonstrate that in that case several conformations are contributing to the overall excitation spectrum. We, therefore, assume that the same will be the case for *trans*-resveratrol. This could in part also explain the rising background as arising from spectral congestion. We can exclude that the underlying reason for the background signal is saturation as the result of too high laser intensities, because the R2PI excitation spectrum of *trans*-resveratrol-3OMe that will be discussed below has been obtained under similar excitation conditions and does not show this broad background.

An alternative reason for the rising background could be that at higher energies higher lying electronically excited states start to contribute to the excitation spectrum. Table 2 reports to this purpose vertical and adiabatic excitation energies calculated for the lowest energy conformer of *trans*-resveratrol. This table shows an excellent agreement between predicted and observed adiabatic excitation energies of the first excited singlet state. At the same time, it shows that the adiabatic excitation energy of  $S_2$  is higher by more than  $4000 \text{ cm}^{-1}$  and, even more importantly, that the  $S_2 \leftarrow S_0$  transition has an oscillator strength that is more than ten times smaller than the transition to  $S_1$ . We thus conclude that higher lying electronically excited states do not contribute to the excitation spectrum shown in Figs. 2 and 4.

A final explanation for the broad background is that it is caused by hydrated *trans*-resveratrol clusters. Trace amounts of water vapor are hard to avoid, and with *trans*-resveratrol featuring three hydroxy groups such clusters are easy to generate. Fragmentation of such clusters upon ionization can then lead to their showing up in the *trans*-resveratrol mass channel monitored in Figs. 2 and 4, and give rise to the broad background. We have tried to obtain further support for the presence of such clusters by monitoring the pertaining mass channels, but these efforts have not been successful. Pump-probe experiments discussed below, as well as the observation that such a background is absent in the ( $1 + 1'$ ) R2PI excitation spectrum of *trans*-resveratrol-3OMe (vide infra)—for which hydrated clusters are much harder to form—lead us, however, to conclude that hydrated clusters contribute to a large extent to the broad background.

Figure 3a shows the decay curve recorded for *trans*-resveratrol after excitation at  $30,664.0 \text{ cm}^{-1}$  the lowest energy band observed in the excitation spectrum of Fig. 2. Decay curves recorded at several other resonances are quite similar.

**Table 2** Vertical and adiabatic TD-DFT excitation energies (eV) of the lower electronically excited states of the lowest energy conformation of *trans*-resveratrol (4a) and *trans*-resveratrol-3OMe (1b) obtained at the wb97XD/cc-pVDZ level with oscillator strengths given in parentheses

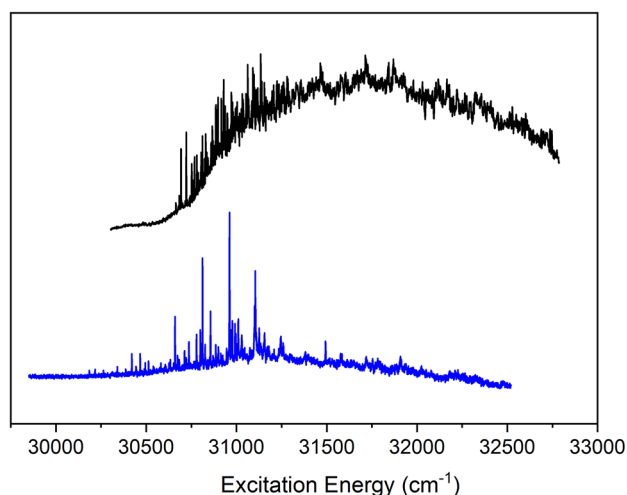
	<i>Trans</i> -resveratrol (4a)		<i>Trans</i> -resveratrol-3OMe (1b)	
	Vertical	Adiabatic	Vertical	Adiabatic
S <sub>1</sub> ( $\pi\pi^*$ )	4.27 (1.00)	3.72 (0.94) <sup>(a)</sup>	4.21 (1.04)	3.69 (1.00)
S <sub>2</sub> ( $\pi\pi^*$ )	4.59 (0.03)	4.26 (0.06)	4.63 (0.04)	4.29 (0.07)
S <sub>3</sub> ( $\pi\pi^*$ )	4.87 (0.07)	4.61 (0.10)	4.87 (0.07)	<sup>(b)</sup>

<sup>a</sup>Under C<sub>s</sub> geometry optimization conditions the harmonic force field gives rise to an imaginary frequency. Geometry optimization along the associated out-of-plane mode does not lead to a stable minimum

<sup>b</sup>During geometry optimization, the root switches with S<sub>2</sub>

Interestingly, we observe a clear bi-exponential behaviour with decay times of 9 and 57 ns. We attribute the 9 ns contribution to the radiative decay of S<sub>1</sub>. This rate is in line with what would be expected on the basis of the rate of (2.7 ns)<sup>-1</sup> as determined for *trans*-stilbene in fluorescence excitation studies when excited at its S<sub>1</sub> ← S<sub>0</sub> 0–0 transition [26]. Such a conclusion is, moreover, supported by TC-SPC studies of the decay of the emission of *trans*-resveratrol-3OMe dissolved in ethanol (vide infra) which find a contribution to the decay of the emission with a decay time of 6 ns. In view of the fact that these TC-SPC measurements do not show addition nanosecond decays, we can rule out the possibility that the 57 ns decay is associated with another conformer of *trans*-resveratrol.

A possible explanation might be that this component derives from a non-emissive electronic state, which would then be the lowest excited triplet state. However, previous solution-phase studies do not find any indication for inter-system crossing [20, 21], and thus seem to rule out such an explanation. Above we have argued that hydrated clusters of *trans*-resveratrol could very well contribute to the R2PI signal. The long-time component can then elegantly be explained as being associated with the excited-state decay

**Fig. 4** (1 + 1') R2PI excitation spectra of *trans*-resveratrol (black) and *trans*-resveratrol-3OMe (blue) (color figure online)

of such a cluster. It is interesting—and requiring further consideration—to notice that this would imply that hydration decreases the radiationless decay rate of S<sub>1</sub> of *trans*-resveratrol by an order of magnitude. However, similar observations have been made for water complexes of phenol [30–32] for which it was argued that changes in the OH stretch frequency in the complex lead to an increase of the observed lifetime from 2 to 15 ns. These observations thus well support the present results.

Figure 4 reports the (1 + 1') R2PI excitation spectrum of *trans*-resveratrol-3OMe and compares it with the spectrum recorded for *trans*-resveratrol over a much more extended energy range. Similar to *trans*-resveratrol this spectrum shows extensive vibronic activity over a large range of excitation energies, featuring sharp bands with widths that are similar to the ones found for *trans*-resveratrol (1.3 cm<sup>-1</sup>). The lowest energy band observed in the spectrum of *trans*-resveratrol-3OMe is found at 30,184.6 cm<sup>-1</sup>, implying a red shift of about 480 cm<sup>-1</sup> compared to *trans*-resveratrol and indicating that the methoxy groups have a larger influence on the electronic structure of the parent compound *trans*-stilbene than the hydroxy groups. Quantum chemical calculations of excitation energies in these two compounds (Table 2) find indeed a slight red shift of the vertical and adiabatic excitation energies for *trans*-resveratrol-3OMe thereby confirming the experimental observations.

In the case of *trans*-resveratrol we suspected that the observed excitation spectrum contained contributions from several conformers but could not find further support for this conclusion, because it was not possible to perform depletion spectroscopy. Table 1 demonstrates that also *trans*-resveratrol-3OMe has several low-energy conformers. Because heating this compound leads to high enough vapor pressures, considerably better signal-to-noise ratios can be obtained, thereby allowing for the successful application of depletion spectroscopy. As yet, only the initial part of the R2PI excitation spectrum has been studied. Nevertheless, the depletion spectra displayed in Fig. 5 that have been obtained for excitation at 30,184.6, 30,216.0, and 30,420.1 cm<sup>-1</sup> clearly show the presence of several distinguishable conformers in the molecular beam. We thus conclude that for *trans*-resveratrol

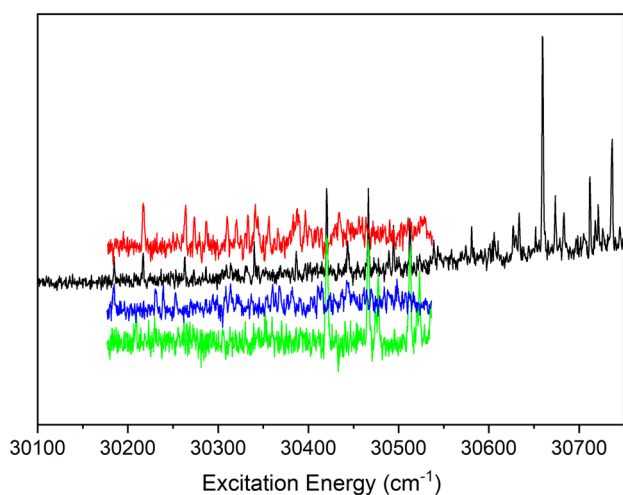


**Fig. 5** Zoom-in of the initial part of R2PI excitation spectrum of *trans*-resveratrol-3OMe (black) combined with UV–UV depletion spectra obtained for excitation at 30,184.6 (blue), 30,216.0 (red), and 30,420.1 (green)  $\text{cm}^{-1}$  (color figure online)

it is also to be expected that more than one conformer contributes to the R2PI excitation spectrum. It will be of interest to extend these studies and investigate whether and to what extent the R2PI excitation spectra show conformer-dependent Franck–Condon activities as was observed, for example, in our studies on sinapate esters [33].

The decay of the ion signal of *trans*-resveratrol-3OMe obtained after excitation at  $30,184.6 \text{ cm}^{-1}$  is displayed in Fig. 3b. Interestingly—and in contrast to *trans*-resveratrol—this decay only shows a mono-exponential decay. Referring once again to TC-SPC measurements on *trans*-resveratrol-3OMe dissolved in ethanol that will be discussed later in which a 6.1 ns component is observed, we assign the 7 ns decay under molecular beam conditions to the decay of  $S_1$ . The absence of a component with a longer decay time is in line with our assignment of this component to hydrated clusters as they are much harder to form in *trans*-resveratrol-3OMe as is, furthermore, corroborated by the absence of a broad background in the excitation spectrum of this compound.

### 3.2 Studies under solvation conditions

Above we have studied spectroscopy and excited-state dynamics of *trans*-resveratrol and *trans*-resveratrol-3OMe under isolated conditions and at low internal temperatures. Applications of resveratrol and its derivatives as sunscreen filters would be done under non-isolated conditions and at room temperature. It is, therefore, key to study the photophysics and photochemistry of these compounds as well under such conditions. To this purpose we have performed two kinds of additional experiments. In the first, the

time-resolved excited-state dynamics have been studied for solutions of these compounds in ethanol, while in the second, it has been determined to what extent such samples degrade when irradiated for a longer time.

The decay of the emission observed for a  $6.0 \times 10^{-6} \text{ M}$  solution of *trans*-resveratrol-3OMe dissolved in ethanol is shown in Fig. 6 together with the Instrument Response Function (IRF). Fitting this decay leads to the conclusion that it shows a biexponential decay with time constants of 32 ps and 6.1 ns and relative contributions of these decays of 0.989 and 0.011, respectively. The time constant of 32 ps is in line with what is expected from the previously reported transient absorption studies on *trans*-resveratrol for which decay times of 19.6 and 28.6 ps were reported for solutions in methanol and acetonitrile, respectively [20, 21]. Importantly, both studies did not report a second decay component, but this could very well be due to the fact that a very high signal-to-noise ratio would be needed to observe the nano-second contribution. In TC-SPC studies on *trans*-resveratrol in various solvents, on the other hand, small ns contributions to the decay of the emission were observed [19].

The present observation of an—albeit quite small—contribution to the decay of the emission of *trans*-resveratrol-3OMe on a much longer time scale is interesting and noteworthy. Our previously described experiments under molecular beam conditions are in this respect quite informative as they show for vibrational levels near the energy minimum in the electronically excited state a decay on the ns timescale that matches the ns decay time observed in solution. We, therefore, attribute the ns decay in solution to molecules in excited-state vibrational levels near the energy minimum, and the ps decay to molecules in vibrational energy levels higher up in the excited state. Such a conclusion implies that there is an energy barrier in the excited state for accessing a decay channel that enables rapid internal conversion to the ground state. In view of the photochemical properties of *trans*-stilbene, we associate this channel with *trans*–*cis* isomerization.

The photochemistry of *trans*-resveratrol in solution under CW irradiation conditions has been extensively studied in the past [14]. As shown in Fig. 7a, irradiation of this compound leads initially to an absorption spectrum with a blue-shifted absorption band around 300 nm that derives from the *cis*-isomer and a red-shifted 350–400 nm absorption band that has been identified as being associated with the highly fluorescent resveratrone compound [34]. We also observe that prolonged irradiation leads to an overall reduction of the entire absorption spectrum which we associate with further degradation of *trans*-resveratrol and the initially photochemically formed species. Further experiments are needed to determine whether this is due to a too-high laser intensity or intrinsic to the photochemistry of *trans*-resveratrol and

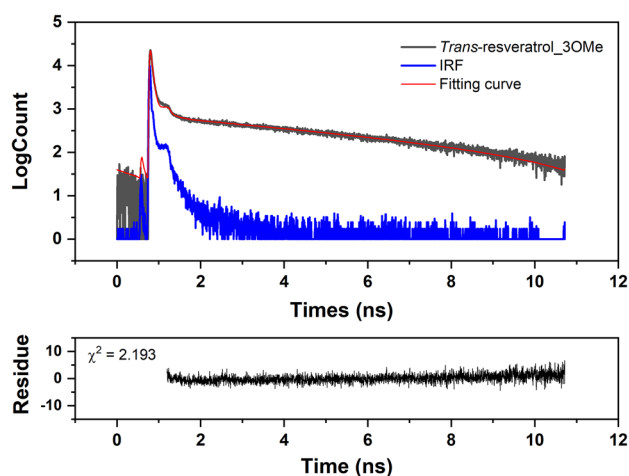


**Fig. 6** Emission decay of *trans*-resveratrol-3OMe dissolved in ethanol concentration of  $6.0 \times 10^{-6}$  M and excitation at 318 nm by collecting emission region of 343–383 nm. The blue trace depicts the Instrument Response Function (IRF), while the red trace is a fit of the decay to the convolution of the IRF with a biexponential decay

its products. The appearance of several other photoproducts in the study of [14] suggests that the latter may well be the case. Clearly, however, both the initially observed and subsequent photochemical transformations are not favorable for sunscreen applications.

The reaction mechanism that has been suggested for the photochemical generation of resveratrone includes several tautomerization steps involving the hydroxy groups. With respect to this particular photodegradation pathway *trans*-resveratrol-3OMe could be a promising alternative, since it does not allow for such tautomerization steps. Although Fig. 7b shows that irradiation still leads to—in this case weakly- fluorescent products with a red-shifted absorption spectrum but to a considerably less extent. We have

tried to identify these products using NMR but these spectra only show the appearance of the *cis* isomer as is also clearly visible in the absorption spectrum. Figure 7b shows that—similar to *trans*-resveratrol—prolonged irradiation of *trans*-resveratrol-3OMe leads to further photochemical degradation, and maybe even more so than in *trans*-resveratrol. In addition, in this case it would be worthwhile to further investigate the pathways along which this occurs similar to what has been done in refs. [14] and [35].

## 4 Conclusions

The present molecular beam studies have allowed for the observation of excitation spectra of the  $S_1 \leftarrow S_0$  transition of *trans*-resveratrol responsible for the UV filtering properties of this compound. While previous studies only reported a very small part of this spectrum, we have here extended it to the entire range from 330 to 300 nm. Analogous to *trans*-stilbene, its parent chromophore, the excitation spectrum shows initially well-resolved vibronic bands that reflect the activity of low-frequency torsional modes, but at higher energies a broadening and coalescing of bands occurs. We have concluded that this could partly be due to the presence of several low-energy conformers in the molecular beam, but certainly also to overcoming a barrier for *trans*–*cis* isomerisation in the excited state. Pump-probe studies show dynamics that are both qualitatively and quantitatively in line with the radiative properties of *trans*-stilbene. In these studies dynamics are also observed on longer time scales, which have been argued to be associated with the excited-state decay of clusters of *trans*-resveratrol with water molecules.

Similar high-resolution studies have been performed on *trans*-resveratrol-3OMe, a derivative that was synthesized to

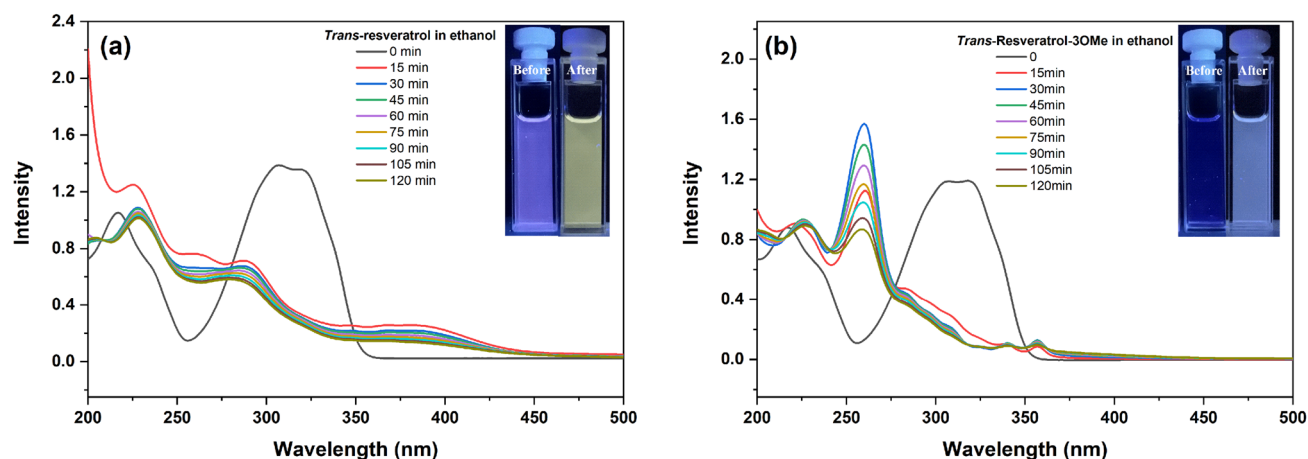


**Fig. 7** UV absorption spectra of (a) *trans*-resveratrol and (b) *trans*-resveratrol-3OMe in ethanol at a concentration of  $6.0 \times 10^{-6}$  M following irradiation at 318 nm



explore the possibility that some of the previously reported photochemical degradation pathways of *trans*-resveratrol would be inhibited. The excitation spectrum of this compound mirrors to a large extent the one observed for *trans*-resveratrol albeit that it is displaced to lower excitation energies. Since upon replacing hydroxy by methoxy groups the formation of clusters with water molecules is less likely, the excitation spectrum is relatively background free—even though depletion spectroscopy explicitly demonstrates that the excitation spectrum has contributions from several conformers—and only monoexponential dynamics are observed.

Finally, a first step has been set to studies under ‘as used’ conditions for sunscreen applications, that is, in solution and at room temperature. These studies confirmed the presence of a radiative excited-state decay channel on the ns time scale, but also—and much more prominent—a decay of the ps timescale that we attributed to photoisomerization. These studies also confirmed that *trans*-resveratrol is photochemically rather labile with *trans*–*cis* isomerization coming prominently forward, and extended UV irradiation leading to extensive photodegradation. Similar observations were made for the *trans*-resveratrol-3OMe derivative, although in that case quite probably other reaction pathways are involved.

Our studies have led to new insight into the photophysics and photochemistry of resveratrol. From a sunscreen application point of view it is clear that further work is required to come to resveratrol-based compounds with an improved and more favourable photochemical profile. The present work is a first step in that direction.

**Acknowledgements** We gratefully acknowledge one of the reviewers who pointed out that hydrated clusters might contribute to the (1+1') R2PI spectrum of *trans*-resveratrol which led to an important re-evaluation of these experiments. We thank ing. Michiel Hilbers and dr. Wim Roeterdink for technical support. Jiayun Fan acknowledges a doctoral fellowship from the China Scholarship Council (No. 201808440365).

**Funding** This project has received funding from the European Union's Horizon 2020 research and innovation programme under the grant agreement No. 828753.

**Data availability** The data sets generated during and/or analysed during the current study are available from the corresponding author on reasonable request.

## Declarations

**Conflict of interest** The authors declare no competing financial interest.

**Open Access** This article is licensed under a Creative Commons Attribution 4.0 International License, which permits use, sharing, adaptation, distribution and reproduction in any medium or format, as long as you give appropriate credit to the original author(s) and the source, provide a link to the Creative Commons licence, and indicate if changes were made. The images or other third party material in this article are included in the article's Creative Commons licence, unless indicated otherwise in a credit line to the material. If material is not included in

the article's Creative Commons licence and your intended use is not permitted by statutory regulation or exceeds the permitted use, you will need to obtain permission directly from the copyright holder. To view a copy of this licence, visit <http://creativecommons.org/licenses/by/4.0/>.

## References

1. Takaoka, M. (1939). Resveratrol, a new phenolic compound, from *veratrum grandiflorum*. *Journal of Chemistry Society. Japan.*, 60, 1090–1100.
2. Wang, Y., Catana, F., Yang, Y. N., Roderick, R., & van Breemen, R. B. (2002). An LC-MS method for analyzing total resveratrol in grape juice, cranberry juice, and in wine. *Journal of Agricultural and Food Chemistry*, 50, 431–435. <https://doi.org/10.1021/jf010812u>
3. Jang, M., Cai, L. N., Udeani, G. O., Slowing, K. V., Thomas, C. F., Beecher, C. W., Fong, H. H. S., Farnsworth, N. R., Kinghorn, A. D., Mehta, R. G., Moon, R. C., & Pezzuto, J. M. (1997). Cancer chemopreventive activity of resveratrol, a natural product derived from grapes. *Science*, 275, 218–220. <https://doi.org/10.1126/science.275.5297.21>
4. Cheng, C. K., Luo, J. Y., Lau, C. W., Chen, Z. Y., Tian, X. Y., & Huang, Y. (2020). Pharmacological basis and new insights of resveratrol action in the cardiovascular system. *British Journal of Pharmacology*, 177, 1258–1277. <https://doi.org/10.1111/bph.14801>
5. Surh, Y. J., Hurh, Y. J., Kang, J. Y., Lee, E., Kong, G., & Lee, S. J. (1999). Resveratrol, an antioxidant present in red wine, induces apoptosis in human promyelocytic leukemia (HL-60) cells. *Cancer Letters*, 140, 1–10. [https://doi.org/10.1016/S0304-3835\(99\)00039-7](https://doi.org/10.1016/S0304-3835(99)00039-7)
6. Asensi, M., Medina, I., Ortega, A., Carretero, J., Baño, M. C., Obrador, E., & Estrela, J. M. (2002). Inhibition of cancer growth by resveratrol is related to its low bioavailability. *Free Radical Biology and Medicine*, 33, 387–398. [https://doi.org/10.1016/S0891-5849\(02\)00911-5](https://doi.org/10.1016/S0891-5849(02)00911-5)
7. Soleas, G. J., Grass, L., Josephy, P. D., Goldberg, D. M., & Diamandis, E. P. (2002). A comparison of the anticarcinogenic properties of four red wine polyphenols. *Clinical Biochem*, 35, 119–124. [https://doi.org/10.1016/S0009-9120\(02\)00275-8](https://doi.org/10.1016/S0009-9120(02)00275-8)
8. Singh, A. P., Singh, R., Verma, S. S., Rai, V., Kaschula, C. H., Maiti, P., & Gupta, S. C. (2019). Health benefits of resveratrol: evidence from clinical studies. *Medicinal Research Reviews*, 39, 1851–1891. <https://doi.org/10.1002/med.21565>
9. Gülçin, I. (2010). Antioxidant properties of resveratrol: A structure–activity insight. *Innovative Food Science Emerging Technologies*, 11, 210–218. <https://doi.org/10.1016/j.ifset.2009.07.002>
10. Orallo, F. (2006). Comparative studies of the antioxidant effects of *cis*- and *trans*-resveratrol. *Current Medicinal Chemistry*, 13, 87–98.
11. Thompson, A. J., Hart-Cooper, W. M., Cunniffe, J., Johnson, K., & Orts, W. J. (2021). Safer sunscreens: Investigation of naturally derived UV absorbers for potential use in consumer products. *ACS Sustainable Chemistry and Engineering*, 9, 9085–9092. <https://doi.org/10.1021/acssuschemeng.1c02504>
12. Aziz, M. H., Afaq, F., & Ahmad, N. (2005). Prevention of ultraviolet-B radiation damage by resveratrol in mouse skin is mediated via modulation in survivin. *Photochemistry and Photobiology*, 81, 25–31. <https://doi.org/10.1111/j.1751-1097.2005.tb01518.x>
13. Freitas, J. V., Lopes, N. P., & Gaspar, L. R. (2015). Photostability evaluation of five UV-filters, *trans*-resveratrol and *beta*-carotene

- in sunscreens. *European Journal of Pharmaceutical Sciences*, 78, 79–89. <https://doi.org/10.1016/j.ejps.2015.07.004>
14. Rodríguez-Cabo, T., Rodríguez, I., Ramil, M., & Cela, R. (2015). Comprehensive evaluation of the photo-transformation routes of *trans*-resveratrol. *Journal of Chromatography A*, 1410, 129–139. <https://doi.org/10.1016/j.chroma.2015.07.088>
  15. Wenzel, E., & Somoza, V. (2005). Metabolism and bioavailability of *trans*-resveratrol. *Molecular Nutrition Food Research*, 49, 472–481. <https://doi.org/10.1002/mnfr.200500010>
  16. Patel, K. R., Scott, E., Brown, V. A., Gescher, A. J., Steward, W. P., & Brown, K. (2011). Clinical trials of resveratrol. *Annals of the New York Academy of Sciences*, 1215, 161–169. <https://doi.org/10.1111/j.1749-6632.2010.05853.x>
  17. Walle, T. (2011). Bioavailability of resveratrol. *Annals of the New York Academy of Sciences*, 1215, 9–15. <https://doi.org/10.1111/j.1749-6632.2010.05842.x>
  18. Callahan, M. P., Gengeliczki, Z., & de Vries, M. S. (2008). Resonant two-photon ionization mass spectrometry of jet-cooled phenolic acids and polyphenols. *Analytical Chemistry*, 80, 2199–2203. <https://doi.org/10.1021/ac7022469>
  19. Simkovitch, R., & Huppert, D. (2015). Excited-state proton transfer in resveratrol and proposed mechanism for plant resistance to fungal infection. *The Journal of Physical Chemistry B*, 119, 11684–11694. <https://doi.org/10.1021/acs.jpcc.5b06440>
  20. Džeba, I., Pedzinski, T., Mihaljević, B., (2015). Photophysical and photochemical properties of resveratrol. *Journal of Photochemistry and Photobiology A: Chemistry*, 299, 118–124. <https://doi.org/10.1016/j.jphotochem.2014.11.019>
  21. Shi, Y. N., Zhao, X. Y., Wang, C., Wang, Y., Zhang, S., Li, P., Feng, X., Jin, B., Yuan, M. H., Cui, S., Sun, Y., Zhang, B., Sun, S., Jin, X., Wang, H., & Zhao, G. (2020). Ultrafast nonadiabatic photoisomerization dynamics mechanism for the UV photoprotection of stilbenoids in grape skin. *Chemistry An Asian Journal*. <https://doi.org/10.1002/asia.202000219>
  22. Irimia, D., Dobrikov, D., Kortekaas, R., Voet, H., van den Ende, D. A., Groen, W. A., & Janssen, M. H. (2009). A short pulse (7 μs FWHM) and high repetition rate (dc-5kHz) cantilever piezovalve for pulsed atomic and molecular beams. *Review of Scientific Instruments*, 80(11). <https://doi.org/10.1063/1.3263912>
  23. Suhina, T., Weber, B., Carpentier, C. E., Lorincz, K., Schall, P., Bonn, D., & Brouwer, A. M. (2015). Fluorescence microscopy visualization of contacts between objects. *Angewandte Chemie International Edition*, 127, 3759–3762. <https://doi.org/10.1002/anie.201410240>
  24. Chai, J. D., & Head-Gordon, M. (2008). Long-range corrected hybrid density functionals with damped atom-atom dispersion corrections. *Physical Chemistry Chemical Physics*, 10, 6615–6620. <https://doi.org/10.1039/B810189B>
  25. M. J. Frisch et al. Gaussian16. Revision C. 01. Gaussian Inc., Wallingford, CT, USA, 2016.
  26. Syage, J. A., Felker, P. M., & Zewail, A. H. (1984). Picosecond dynamics and photoisomerization of stilbene in supersonic beams. I. Spectra and mode assignments. *The Journal of Chemical Physics*, 81, 4685–4705. <https://doi.org/10.1063/1.447519>
  27. Renge, I. (2000). Mechanisms of solvent shifts, pressure shifts, and inhomogeneous broadening of the optical spectra of dyes in liquids and low-temperature glasses. *The Journal of Physical Chemistry A*, 104, 7452–7463. <https://doi.org/10.1021/jp000176n>
  28. Chiang, W. Y., & Laane, J. (1994). Fluorescence spectra and torsional potential functions for *trans*-stilbene in its S<sub>0</sub> and S<sub>1</sub>(<sup>\*</sup>) electronic states. *The Journal of Chemical Physics*, 100, 8755–8767. <https://doi.org/10.1021/j100031a006>
  29. Orlandi, G., Garavelli, M., & Zerbetto, F. (2017). Analysis of the vibronic structure of the *trans*-stilbene fluorescence and excitation spectra: The S<sub>0</sub> and S<sub>1</sub> PES along the C<sub>e</sub>=C<sub>e</sub> and C<sub>e</sub>-C<sub>ph</sub> torsions. *Physical Chemistry Chemical Physics*, 19, 25095–25104. <https://doi.org/10.1039/C7CP01594A>
  30. Sur, A., Johnson, P.M., (1986). Radiationless transitions in gas phase phenol and the effects of hydrogen bonding. *The Journal of Chemical Physics*, 84, 1206–1209 (1986). <https://doi.org/10.1063/1.450512>
  31. Lipert, R.J., Bermudez, G., Colson, S.D. (1988). Pathways of S<sub>1</sub> decay in phenol, indoles, and water complexes of phenol and indole in a free jet expansion *The Journal of Physical Chemistry*, 92, 3801–3805. <https://doi.org/10.1021/j100324a024>
  32. Lipert, R. J., & Colson, S. D. (1990). Time-resolved pump-probe photoionization study of excited-state dynamics of phenol-(H<sub>2</sub>O)<sub>2</sub> and Phenol-(H<sub>2</sub>O)<sub>3</sub>. *The Journal of Physical Chemistry*, 94, 2358–2361. <https://doi.org/10.1021/j100369a031>
  33. Fan, J., Roeterdink, W., Buma, W. J. (2021). Excited-state dynamics of isolated and (micro) solvated methyl sinapate: The bright and shady sides of a natural sunscreen. *Molecular Physics*, 119, e1825850. <https://doi.org/10.1080/00268976.2020.1825850>
  34. Yang, I., Kim, E., Kang, J., Han, H., Sul, S., Park, S. B., & Kim, S. K. (2012). Photochemical generation of a new, highly fluorescent compound from non-fluorescent resveratrol. *Chemical Communications*, 48, 3839–3841. <https://doi.org/10.1039/C2CC30940H>
  35. Vink, M. J. A., Schermer, J. J., Martens, J., Buma, W. J., Berden, G., & Oomens, J. (2023). Characterization of solar radiation-induced degradation products of the plant sunscreen sinapoyl malate. *ACS Agricultural Science & Technology*, 3, 171–180. <https://doi.org/10.1021/acscagcitech.2c00279>